Fuel 103 (2013) 814–826

Contents lists available at SciVerse ScienceDirect

Fuel

journal homepage: www.elsevier.com/locate/fuel

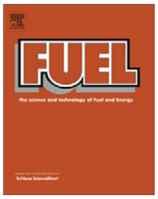

Torrefaction of ionic-liquid impregnated lignocellulosic biomass and its comparison to dry torrefaction

A. Sarvaramini, O. Gravel, F. Larachi *

Department of Chemical Engineering, Laval University, Québec, QC, Canada G1V 0A6

HIGHLIGHTS

- ▶ Woody biomass torrefaction impregnated with room-temperature ionic liquids.
- ▶ Biochar energy density in ionic-liquid torrefaction outperforms dry torrefaction.
- ▶ Biomass ash leftovers catalyze ionic liquid degradation.
- ▶ Ionic liquid torrefaction improves biochar hydrophobicity.
- ▶ Ionic liquid torrefaction reduces biochar water uptake.

ARTICLE INFO

Article history:
Received 24 April 2012
Received in revised form 13 September 2012
Accepted 15 September 2012
Available online 3 October 2012

Keywords:
Biomass treatment
Lignocellulosic biomass
Torrefaction
Ionic liquid
Stability

ABSTRACT

Torrefaction of woody biomass as a thermal pretreatment to increase biomass energy density is prerequisite to many thermochemical conversions. An ionic-liquid (IL) biomass torrefaction route was proposed and investigated as an alternative to conventional dry and wet torrefaction for enhancing the rate of biomass torrefaction and for potentially improving the quality of torrefied solid products. Ionic liquid-impregnated aspen, birch and sawdust were torrefied in the 240–280 °C temperature range using [Emim][OTf], [Emim][BF_4] and [Hmim][NTf_2] ILs. To assess the benefits of IL impregnated biomass, dry and IL torrefaction were compared in terms of mass yield, energy density, energy yield, hydrophobicity and ultimate moisture uptake of torrefied solid products using thermogravimetry and fixed-bed setups. At equal reaction time and treatment temperature, the decomposition rates of birch, aspen and sawdust in ILs were considerably enhanced compared to their dry torrefaction counterparts. IL torrefaction led to increased energy density of treated aspen, birch and sawdust solids alike, whereas improved hydrophobicity of IL-torrefied solids translated in nearly 40–45% reduction of their ultimate moisture uptake. Finally, char and ash leftovers building up in spent ILs after repeated IL torrefaction cycles were specifically addressed as potential factors responsible for IL decomposition.

© 2012 Elsevier Ltd. All rights reserved.

1. Introduction

Biomass as a carbon-neutral renewable energy source is increasingly receiving attention for the essential role it is anticipated to play in the world's energy [1]. However, raw biomass as a fuel features low calorific value and high oxygen-to-carbon ratio (O/C), and, being hygroscopic, high moisture besides producing smoke during combustion [2,3]. Dry and wet torrefaction of biomass are the thermal pretreatments often used to attend for these limitations to improve biomass properties [3,4]. Dry torrefaction consists of slowly heating biomass in an inert atmosphere from 200 °C to 300 °C [5]. Wet torrefaction is a hydrothermal pretreatment wherein biomass is subjected to pressurized liquid water up to 5 MPa and 260 °C for ca. 60 min [6,7]. Both processes yield hydrophobic solid products with lower moisture content and O/C ratio, and higher energy density than raw biomass making them suitable biofuels [6–10]. Though at the expense of an elevated pressure, wet torrefaction produces solids with energy density greater than dry torrefaction [6]. To limit tar production and maximize energy for a given mass yield, dry biomass torrefaction requires capping temperatures below 300 °C. Also, depending on biomass particle sizes, the residence time required for dry torrefaction varies widely, typically from 10 min for finely ground biomass particles to several hours for coarser bits thus all in all reflecting in large variability in reactor sizes [11].

The initial stage in biomass torrefaction involves hemicellulose decomposition which occurs extensively around 250–260 °C [12]. But unlike hemicellulose, lignin and cellulose barely decompose

---

* Corresponding author. Tel.: +1 418 656 3566; fax: +1 418 656 5993.
E-mail address: faical.larachi@gch.ulaval.ca (F. Larachi).

0016-2361/$ - see front matter © 2012 Elsevier Ltd. All rights reserved.
http://dx.doi.org/10.1016/j.fuel.2012.09.037

below these temperatures contributing to a minor mass loss. The second stage in biomass torrefaction involves decomposition of cellulose which is less reactive than hemicellulose and rate-controlling below 300 °C [11]. Water, CO and CO_2 evolve subsequent to the breakdown of hydrogen bonds within or between cellulose molecules resulting in a change in cellulose super-molecular structure shortening its length from 10^4 down to ca. 200 [13]. Increasing torrefaction temperature over 270 °C positively affects the rate of cellulose decomposition [12].

Different classes of solvents such as mineral acids and ionic liquids have proved capable of disrupting the hydrogen bonds between the different polysaccharide chains. Solvent exposure results in decreasing material compactness and in increasing sensitivity to hydrolysis of the carbohydrate fraction [14]. Such features are good omen for testing solvents to host biomass torrefaction. Doping cellulose with mineral acids such as H_2SO_4, HCl and HNO_3 is known to considerably increase the rate of cellulose decomposition and to lower the required decomposition temperature [15]. However, corrosiveness of most acids as well as their volatility, which leads to poisonous emanations [16] at elevated temperatures, make them unappealing for use in biomass torrefaction. Unlike mineral acids, room-temperature ionic liquids (ILs) feature very low vapor pressures, low flammability and high thermal stability [17,18]. ILs are also good heat-transfer media which may be a desirable characteristics to enhance heat transfer around the solid biomass [19]. Consequently, the potential of ionic liquids (ILs) to enhance the rate of biomass torrefaction and to improve the quality of torrefied solid products is worth investigating.

Torrefaction of three woody biomass varieties impregnated with three imidazolium-cation based ILs, namely, [Emim][OTf]: 1-ethyl-3-methyl imidazolium trifluoromethanesulfonate, [Emim][BF_4]: 1-ethyl-3 methylimidazolium tetrafluoroborate and [Hmim][NTf_2]: 1-hexyl-3-methylimidazolium bis(trifluoro methylsulfonyl)imide is studied in this work. These ILs were screened on the basis of biomass dissolution studies at *mild* temperatures which revealed these ionic liquids exhibit weak interactions with biomass [20] in addition to superior thermal stability at the tested torrefaction temperatures (240–280 °C). Imidazolium halide-based ionic liquids, e.g., [Emim][Cl] or [Bmim][Cl], were not considered instead despite their featured superior biomass dissolving power. Too much stimulated biomass solubility by the high torrefaction temperatures was feared to do away with any residual biochar from recovery. Besides halide-bearing ILs showcase a low thermal stability and toxicity preventing their consideration for the present biomass torrefaction experiments [20,21–23]. [Emim][OTf] and [Emim][BF_4] are hydrophilic and their onset decomposition temperature exceeds 400 °C [24]. They also have shown ability to dissolve mono- and disaccharides such as glucose and sucrose [25] owing to hydrogen bond interactions via numerous carbohydrate hydroxyl groups [18]. However, dissolution in these ionic liquids of polysaccharides, such as cellulose, is low at mild temperature (up to 110 °C) due to the presence of large non-coordinating anions and their relatively low hydrogen bond basicities [20]. Unlike [Emim][OTf] and [Emim][BF_4], [Hmim][NTf_2] is hydrophobic with onset decomposition temperatures above 400 °C [26]. [Hmim][NTf_2] has large anion and cation sizes which makes it a poor solvent for cellulose and lignin dissolution [20].

2. Experimental

2.1. Materials

[Emim][OTf], [Emim][BF_4] and [Hmim][NTf_2] ionic liquids with 99% purity were purchased from Io-li-tech. Acidity tests using aqueous 10 vol.% [Emim][OTf] mixtures led to pH = 2.5 revealed the presence of acidic residual impurities in the Io-li-tech ionic liquid. Such acidic impurities may enhance hydrogen bond breakup in the cellulose structure. Hence to distinguish the effects of acidic impurities and ionic liquid itself on biomass torrefaction, [Emim][OTf] free from acidic impurities was also purchased from Sigma Aldrich with purity >98%. The Io-li-tech and Sigma ILs are designated as $[Emim][OTf]_I$ and $[Emim][OTf]_s$.

Table 1
Proximate analysis in mass% of sawdust, birch and aspen wood.

	Humidity	Volatile (dry basis)	Fixed carbon (dry basis)	Ash (dry basis)
Sawdust	5.3	79.6	16.1	4.3
Birch	5.5	89.4	9.8	0.7
Aspen	4.8	87.5	12	0.5

Powdered samples of cellulose (Avicel®PH-101), xylan hemicellulose representative (X0502) and lignin (37059-lignin, alkali), purchased from Sigma Aldrich and three types of woody biomass (trembling aspen, birch and sawdust) were torrefied. The proximate analysis of aspen, birch and sawdust is given in Table 1. The sawdust was in the form of biomass pellets supplied from Enerkem (Québec). This sample was a mixture of different woody biomass residues which is used for gasification purposes. All the samples were first grinded and then sieved to isolate the 1–2 mm particles of sizes. Each biomass type was impregnated with each of the three ionic liquids. Impregnation of biomass with ionic liquid was carried out under mixing at 60 °C to maximize ionic liquid absorption while preventing biomass dissolution [20]. The biomass samples were weighted regularly to estimate the amount of absorbed ionic liquid. Absorption was dependent on the type of biomass and ionic liquid but was maximum with $[Emim][OTf]_{I,S}$. The mass ratio of absorbed ionic liquid to biomass was in the range 1.5–2, 1.8–2.2 and 1.5–1.9 for birch, aspen and sawdust, respectively, whereas it was fixed to 2 for cellulose, xylan and lignin.

2.2. Weight loss and volatiles via thermogravimetry and mass spectrometry analysis

A thermogravimetric analyzer (TG) (Perkin Elmer Lab System Diamond TGA-DTA) coupled with a quadrupole mass spectrometer (MS) (Thermostar Prisma QMS200, Pfeiffer Vacuum) was used to monitor the weight loss and volatiles released, and the temperature, Ts, at which biomass decomposition starts during IL and dry torrefaction (Fig. SC-1, Supplementary Material). The samples first were dried in TG at 120 °C for 30 min and then submitted to prograde heating at 5 °C/min under N_2 flow (100 N mL/min) until 280 °C where they were maintained for 60 min. The gases released from biomass decomposition were identified via MS. Special care was taken in choosing the sample containers to prevent corrosion by ionic liquids. Three different containers were tested, i.e., aluminum, alumina and platinum. Although aluminum was neutral to [Hmim][NTf_2] and [Emim][OTf], a remarkable corrosion in the presence of [Emim][BF_4] was observed. Aluminum catalyzed the decomposition of BF_4 anions especially in the acidic media leading to the formation of fluoroaluminate complexes [27]. The weight of aluminum container after contacting with [Emim][BF_4] was lower than originally unveiling the corrosive nature of [Emim][BF_4]. No change in the weight of alumina and platinum containers were observed in the presence of all three tested ionic liquids. Also, preliminary ionic liquid high-temperature degradation tests performed in both containers showed unchanged IL degradation rates. Consequently, alumina and platinum containers had no interaction with the tested ILs. Alumina pans owing to a higher capacity were chosen for the experiments.

2.3. Fixed-bed torrefaction setup

As the amount of residual solid products recovered following TG analyses was too low for further quantifications, a fixed-bed torrefaction reactor was designed to obtain sufficient torrefied materials for complementary investigations on solid products. Furthermore, TG analysis revealed a more remarkable effect of [Emim][OTf] on the decomposition rate and T_s for birch, aspen and sawdust woods. Only this latter ionic liquid was tested for the fixed-bed reactor tests. The bench scale torrefaction unit (Fig. 1) consisted of a stainless steel (SS) tube (ID. 34 mm, length 70 cm) placed inside an induction coil. A biomass sample 0.6 g in mass either impregnated with ionic liquid or not (dry torrefaction) was held atop of a steel grid located in the middle of the stainless steel tube to act as a support for the biomass bed. The reactor was heated through a 15 cm long coil connected to a 18 kW induction power supply for heating the stainless steel tube via AC magnetic field then heating in turn the biomass layer through radiation and conduction. The biomass bed temperature was raised from the ambient to the target temperature (240–280 °C) in less than 10 s and then the samples were kept at final temperature for specified time duration (10–60 min). The SS tube temperature was controlled by a fiber optic pyrometer connected to a temperature controller to meter the induction-heater power. Temperature was also measured through a K type thermocouple inserted in the center of the biomass bed. The difference between the bed temperature and SS tube surface at steady state condition never exceeded 5 °C. In order to keep the reactor environment inert and remove the volatiles from the reactor to the cold trap, a continuous flow (100 mL/min) of N_2 passed through the bed. The cold trap consisted of a tube inserted inside a bigger one filled with a 70 mass% ethylene glycol aqueous solution. This was then placed inside a container full of liquid N_2. The freezing point of this aqueous ethylene glycol solution allowed a minimal interior temperature of −55 °C to be reached. This temperature was low enough to ensure maximum separation of condensable gases while sparing CO, CO_2 and methane which were transferred to a gas bag until the completion of the test.

2.4. Characterization of solids

The torrefied biomass was removed from the steel grid, placed on a filter paper and washed for 30 min with approximately 200 mL of distilled water using vacuum filtration. The recovered solid was dried in an oven at 110 °C for 12 h and then weighted to assess the total mass loss. The water and ionic liquid filtrate was once again filtered using syringe filters to remove the smaller solid impurities. The clear solution was subsequently transferred into a flask wherefrom water was evaporated under vacuum in a rotating evaporator with a 120 °C Calflo AF bath. The ionic liquid leftover was then weighted.

Solid products from torrefaction were further analyzed to investigate their properties after thermal treatment. The C, H, N, S sample contents were measured using a Fisons EA 1108CHNS elemental analyzer. All measurements were duplicated and their average was reported. The higher heating value (HHV) of the samples before and after torrefaction was inferred using Friedl et al. equation [28] based on carbon, hydrogen and nitrogen content of biomass. This equation is considered enough robust for such estimations as it was derived on the basis of 122 biomass samples with less than 2 wt.% error [29,30]:

$$\mathrm{HHV\ (kJ/kg)} = 3.55 \cdot C^2 - 232 \cdot C - 2230 \cdot H + 51.2 \cdot C \cdot H + 131 \cdot N + 20,600$$

where C, H and N represent carbon, hydrogen, and nitrogen mass%, respectively.

The effect of torrefaction treatments was evaluated in terms of hydrophobicity, ultimate moisture uptake, U_{MU}, i.e., percent mass water uptake on a dry biomass basis), and contact angle measurements. The ultimate moisture uptakes, U_{MU}, of raw and torrefied biomass samples were obtained by putting 300 mg of the samples in a vapor-saturated bath controlled at 30 °C. To eliminate pre-existing moisture before U_{MU} measurements, all the samples were dried overnight at 110 °C. They then were placed in a bath for 4 days and their weight gain was measured after all the samples

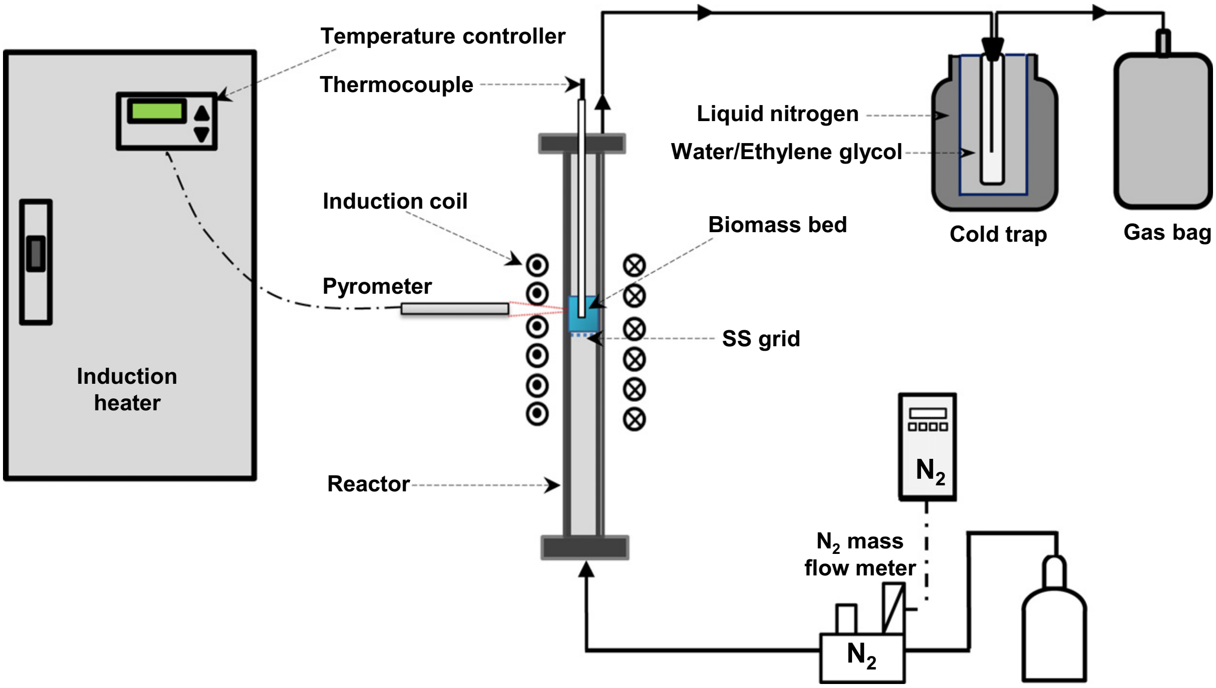

Fig. 1. Schematics of fixed-bed reactor setup used for biomass torrefaction.

reached equilibrium. The water contact angles of raw and torrefied biomass were also measured using an optical contact angle analyzer (OCA 15 EC Plus, Dataphysics) using the sessile drop method. The system employed a high-resolution camera and specific software developed for OCA 15 EC Plus to capture and analyze the contact angle on very small and curved surfaces.

3. Results and discussion

3.1. IL and dry torrefaction, TG–MS studies

IL and dry torrefaction of cellulose, hemicellulose and lignin individual components could shed insights on the mechanisms contributing to biomass torrefaction as these make up, respectively, 55–60 wt.%, 20–25 wt.% and 15–20 wt.% of the biomass samples [31,32]. Moreover, pyrolysis kinetic studies have shown that the rate of biomass decomposition stems from parallel thermal decomposition of each model component [33]. Dry and IL torrefaction of cellulose, hemicellulose and lignin model compounds were performed in TG–MS to determine both T_s and weight loss profiles. A 2:1 IL-to-model component ratio was used in the latter torrefaction tests. The samples were dried in TG at 120 °C for 30 min before their prograde heating at 5 °C/min under 100 N mL/min N_2 flow until 280 °C where they were kept for 1 h.

3.1.1. Torrefaction of model compounds

Cellulose thermal decomposition for both IL and dry torrefaction is shown in Fig. 2. Torrefaction of cellulose in [Emim][OTf]$_S$ and [Emim][OTf]$_I$ led to T_s of 190 and 220 °C, respectively, while T_s for dry torrefaction was much higher at 260 °C. The rate of thermal decomposition of cellulose was also markedly increased in [Emim][OTf]$_I$ and [Emim][BF$_4$]. The time required for dry torrefaction of cellulose to reach 70% of solid product yield was 22 min. Under the applied heating program, this time was reduced to 8 and 10 min, respectively, for cellulose torrefied in [Emim][BF$_4$] and [Emim][OTf]$_I$. Cellulose torrefaction in [Emim][OTf]$_S$ featured a slower decomposition step leading to 28% mass loss and followed by a faster step contributing an additional 51%. Cellulose torrefaction in [Hmim][NTf$_2$], in comparison with dry torrefaction barely altered both the decomposition rate and T_s. Such indifference can be attributed to [Hmim][NTf$_2$] bulkier anions and cations resulting in less efficient interactions with cellulose as compared to [Emim][BF$_4$] and [Emim][OTf].

Acceleration of cellulose torrefaction in [Emim][OTf]$_{I,S}$ and [Emim][BF$_4$] was also corroborated via MS monitoring of CO_2 and H_2O release accompanying mass losses. Fig. 3 shows the evolution of CO_2 during IL and dry torrefaction of cellulose. Pure ionic liquids subjected to the same TG heating program released almost no CO_2. Consequently, the detected CO_2 was plausibly arising from thermal decomposition of cellulose and not from ionic liquids. As observed, CO_2 was released at temperatures as low as 150 °C for cellulose torrefied in [Emim][OTf]$_S$. In both cases of [Emim][OTf]$_I$ and [Emim][BF$_4$], CO_2 release started near 200–210 °C while the onset of CO_2 release for dry torrefaction of cellulose occurred at 260 °C. The rates of CO_2 release from cellulose in [Emim][OTf]$_{I,S}$ and [Emim][BF$_4$] were rather sharp featuring more intense ion current peaks than for cellulose torrefied in [Hmim][NTf$_2$] or in the dry mode. Ion currents corresponding to water released from cellulose also featured the same trend as CO_2, Fig. 4. Torrefaction of cellulose in [Emim][OTf]$_{S,I}$ and [Emim][BF$_4$] drastically increased the amount of water released from cellulose. Water release also started at lower temperatures under [Emim][OTf]$_{S,I}$ and [Emim][BF$_4$] cellulose torrefaction and unlike dry torrefaction.

To investigate how ionic liquids pre-exposed to elevated temperatures affect cellulose decomposition activity, [Emim][OTf]$_S$ was heated at 280 °C for 48 h before it was impregnated on cellulose. The heat-treated ionic liquid is referred to [Emim][OTf]$_{ST}$ and its effect on cellulose decomposition is shown in Fig. 2. As seen, the rate of cellulose decomposition impregnated with [Emim][OTf]$_{ST}$ is as high as cellulose torrefied by [Emim][OTf]$_I$ and [Emim][BF$_4$] while T_s has shifted slowly toward higher temperatures. Heat treatment of [Emim][OTf]$_S$ caused its properties look like [Emim][OTf]$_I$ for cellulose decomposition.

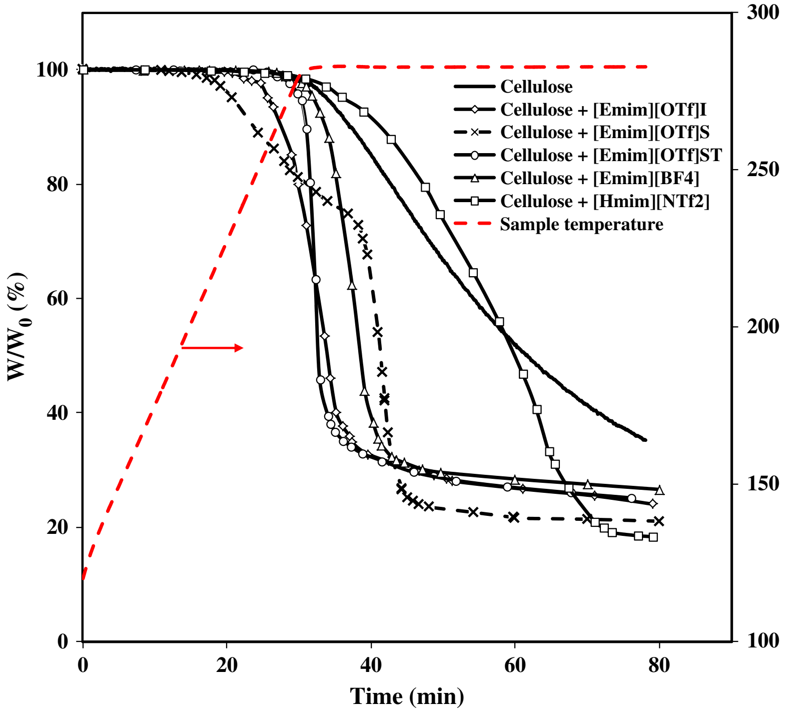

Fig. 2. Mass loss profile of cellulose ionic liquid and dry torrefaction.

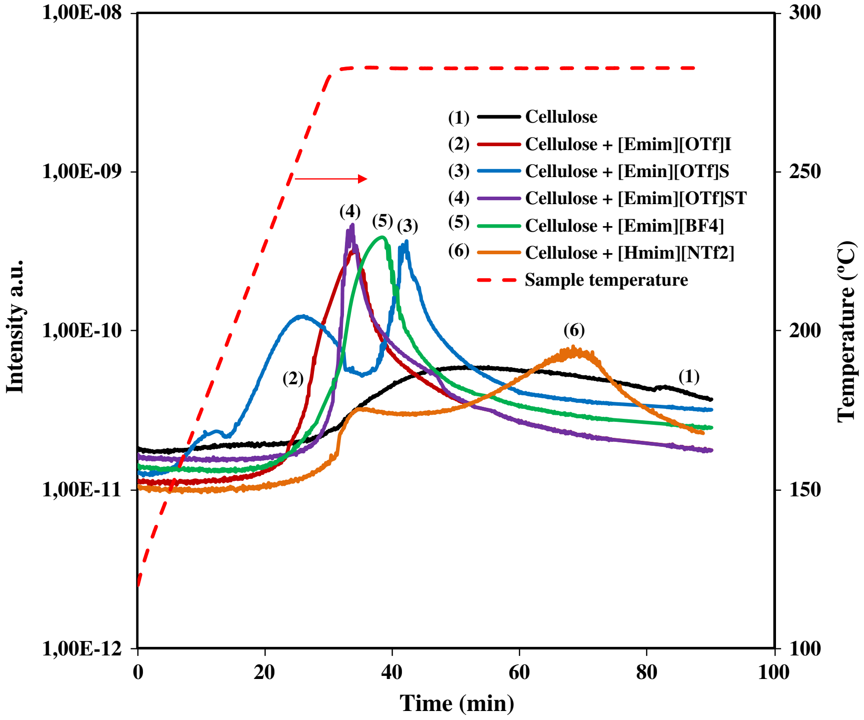

Fig. 3. MS positive ion current ($m/z = 44$, CO_2) during cellulose ionic liquid and dry torrefaction.

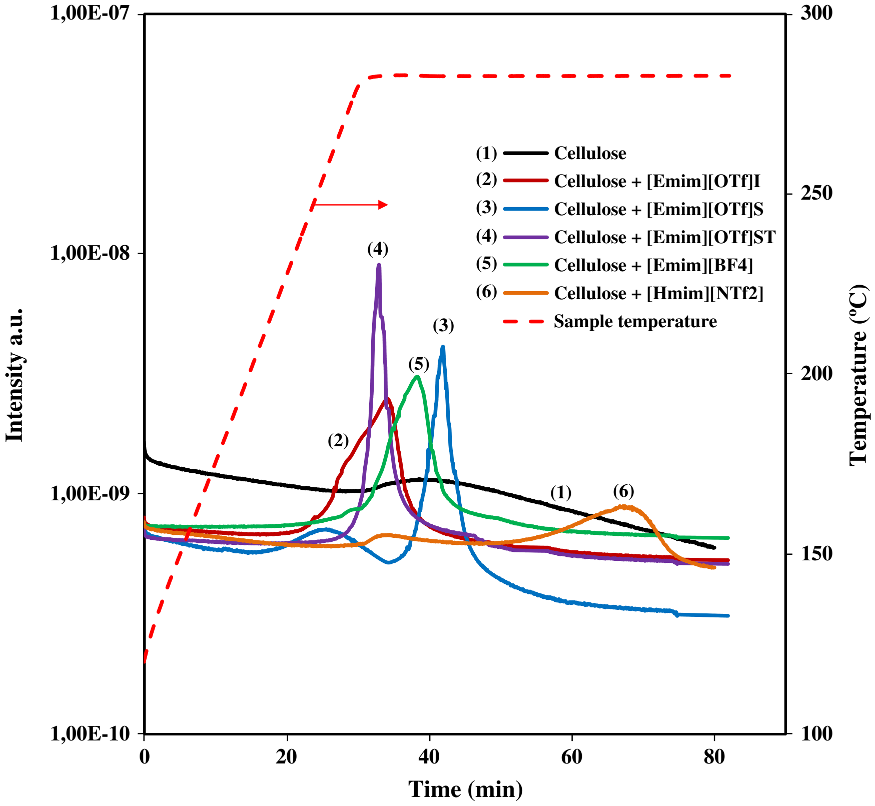

Fig. 4. MS positive ion current ($m/z = 18$, H_2O) during cellulose liquid and dry torrefaction.

Fig. 5 shows xylan decomposition in dry and ionic-liquid torrefaction treatments. Xylan torrefaction in [Emim][OTf]$_S$ started at lower temperatures in comparison with the other ionic liquids or dry with dry torrefaction. However the rate of xylan decomposition did not change remarkably using the different ionic liquids. Ionic liquid torrefaction of xylan also led to more final decomposition than dry torrefaction, Fig. 5. In contrast with cellulose and xylan, ionic-liquid torrefaction of lignin had considerably lower effect

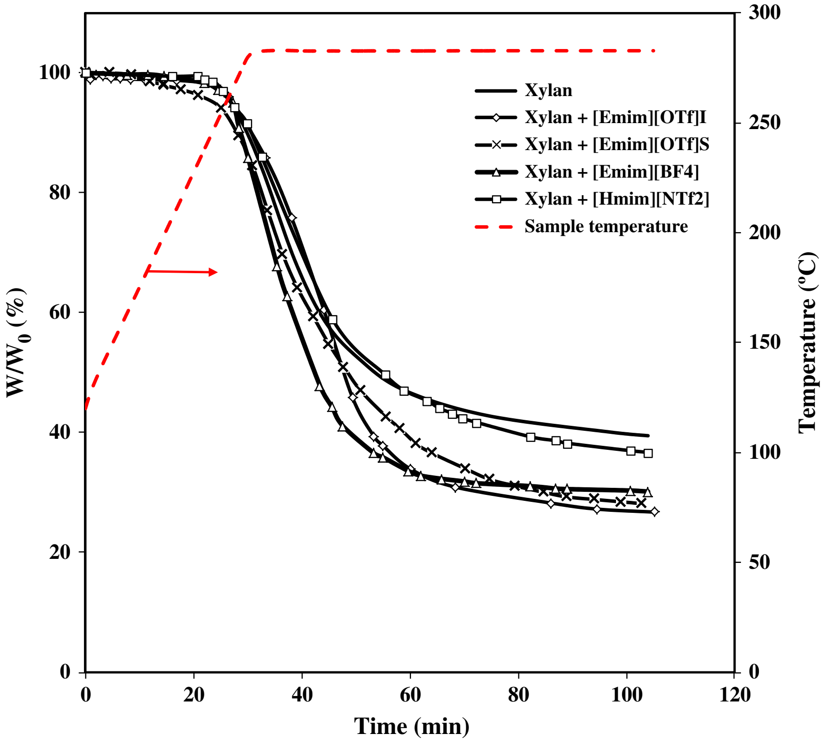

Fig. 5. Mass loss profile of xylan ionic liquid and dry torrefaction.

on its T_s, Fig. 6. The decomposition rate of lignin torrefied by ionic liquids also did not change significantly compared to dry torrefaction lignin. The small increase in the final decomposition of lignin is due to its torrefaction by $[Emim][OTf]_{I,S,ST}$ and $[Emim][BF_4]$.

3.1.2. Torrefaction of woody biomass

IL and dry torrefaction of aspen, birch and sawdust was performed in TG–MS to obtain both T_s and weight loss profiles. Decomposition of aspen, birch and sawdust during IL torrefaction differs in trends from dry torrefied in accordance with the behaviors noted above for their constitutive model components. IL and dry torrefaction of aspen is shown in Fig. 7 featuring an important decrease in T_s in presence of $[Emim][OTf]_{S,I}$. Decomposition of $[Emim][OTf]_{S,I}$-torrefied aspen started as low as 160 °C contrasting with $T_s \sim 200$ °C of dry torrefaction. The rate of aspen decomposition was also quite higher for $[Emim][OTf]_{S,I}$- and $[Emim][BF_4]$-torrefied aspen compared to aspen dry torrefaction. $[Emim][OTf]_I$ torrefaction outperformed that of $[Emim][OTf]_s$ whereby the increased rate of aspen decomposition must have been due to the $[Emim][OTf]_I$ acidic impurities. Regardless of which IL is used, aspen torrefaction led to higher weight losses compared to dry torrefaction for the same contact times. The maximum aspen decomposition occurred with $[Emim][OTf]_s$. Birch wood behaved nearly the same way as shown in Fig. 8. Furthermore, T_s for IL torrefaction of birch wood was lower than in dry torrefaction while birch wood decomposition rates were the slowest with $[Hmim][NTf_2]$. Fig. 9 compares the sawdust mass losses for IL and dry torrefaction. Contrary to dry torrefaction, higher decomposition rates as well as deeper weight losses are observed for sawdust torrefied in $[Emim][OTf]_{I,S}$ and $[Emim][BF_4]$. Also, T_s for $[Emim][OTf]_{S,I}$ and $[Emim][BF_4]$ torrefied sawdust was also lower compared to dry torrefaction of sawdust.

As can be seen in Figs. 7–9, the rate of decomposition of aspen, birch and sawdust could be considerably affected by the sample impregnation with ionic liquids. These latter could effectively disrupt the extensive intra- and inter-molecular hydrogen bonding network in cellulose as well as intermolecular hydrogen bonding between cellulose and lignin leading to a higher decomposition rate of the tested biomass samples [16–18]. The interaction of ionic liquids with lignocellulosic biomass involves hydrogen bonding interactions between ionic liquid and biomass. Consequently, ionic liquids whose anions and cations have strong hydrogen bond accepting ability are more efficient in disrupting cellulose structure [17,18,20]. As can also be observed in Figs. 7–9, impregnated aspen, birch and sawdust by [Emim][OTf], [Emim][BF4] showcase considerably higher decomposition rates than [Hmim][NTf2]-impregnated samples. The cation size of [Hmim][NTf2] is larger than in [Emim][OTf] and [Emim][BF4]. Large cation size of [Hmim][NTf2] reduces its power for disrupting the celluose structure due to lesser ability of large cations to form hydrogen bonds with cellulose [16–18]. Relatively small cations are often efficient in disrupting hydrogen bonds of cellulose, and when the alkyl chain length in the cation increases, as for [Hmim][NTf2], the ability of ionic liquid to interact with lignocellulosic materials is decreasing [20]. However, additional experimental and theoretical studies are still needed to fully explain the effect of the nature of specific anions and cations on the torrefaction of biomass.

3.2. IL and dry biomass torrefaction, fixed-bed studies

The previous TG tests showed that the activity of [Emim][OTf]-mediated TG torrefaction of aspen, birch and sawdust outperformed that from $[Emim][BF_4]$ and $[Hmim][NTf_2]$. Also the presence of acidic impurities in $[Emim][OTf]_I$ were sensed to have some effects on the rate of decomposition of biomass. Consequently, $[Emim][OTf]_S$ which is less prone to active impurities is chosen for the fixed-bed IL torrefaction of aspen, birch and sawdust. IL and dry torrefaction of aspen, birch and sawdust were performed at temperatures between 240 and 280 °C for contact times ranging from 10 to 60 min. The solid biomass products obtained

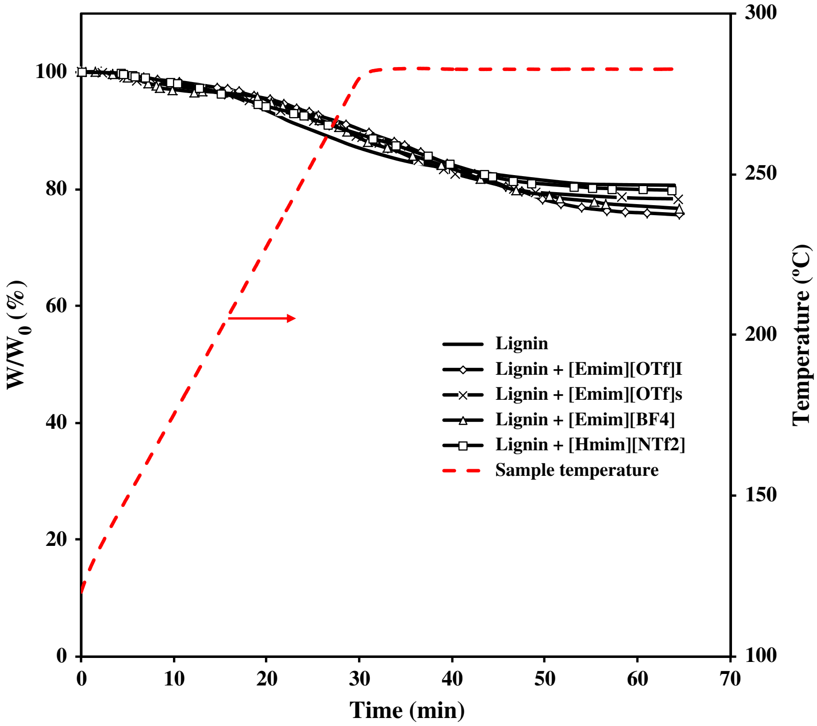

Fig. 6. Mass loss profile of lignin ionic liquid and dry torrefaction.

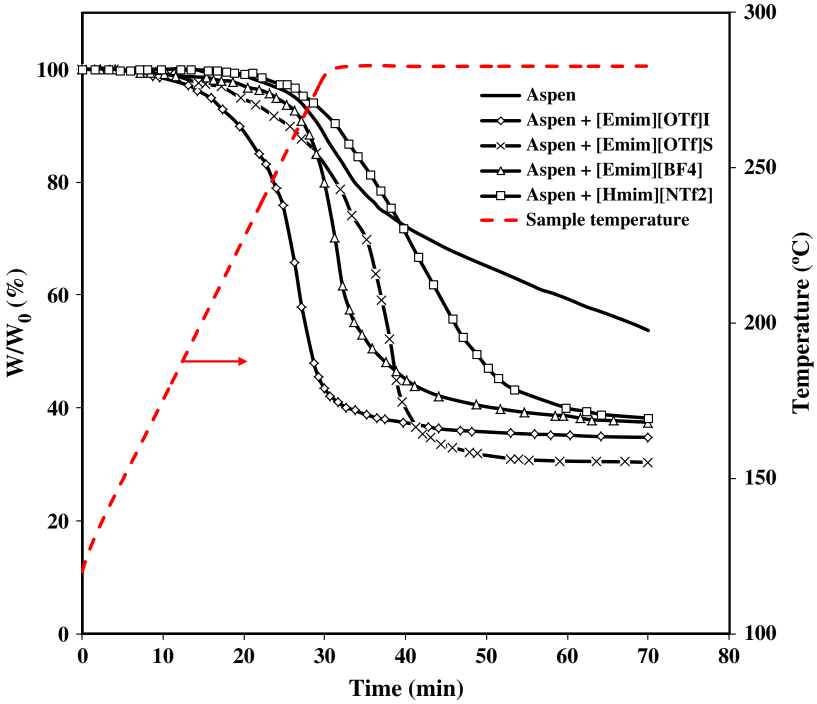

Fig. 7. Mass loss profile of aspen ionic liquid and dry torrefaction.

after dry and IL torrefaction of woody biomass were characterized in terms of mass yield (Y_M = mass% solid product/mass feed), energy density (e = HHV solid product/HHV feed), energy yield ($Y_e = e \cdot Y_M$), ultimate moisture uptake (U_{MU}) and hydrophobicity.

Torrefaction of [Emim][OTf]$_S$-impregnated aspen, birch and sawdust led to brownish solids (Fig. SC-2, Supplementary Material). The torrefied solid products after [Emim][OTf]$_S$ and dry torrefaction of aspen, birch and sawdust are compared in Fig. 10 in terms of their mass yields, Y_M, at different temperatures and contact times. For any given biomass sample, IL-torrefied solids exhibit lower Y_M, in the 58–72% of initial weight, in comparison to those obtained in dry torrefaction, 74–84% of initial weight, everything else being kept constant. Also, irrespective of the type of torrefaction, a lower mass yield of aspen, birch and sawdust was

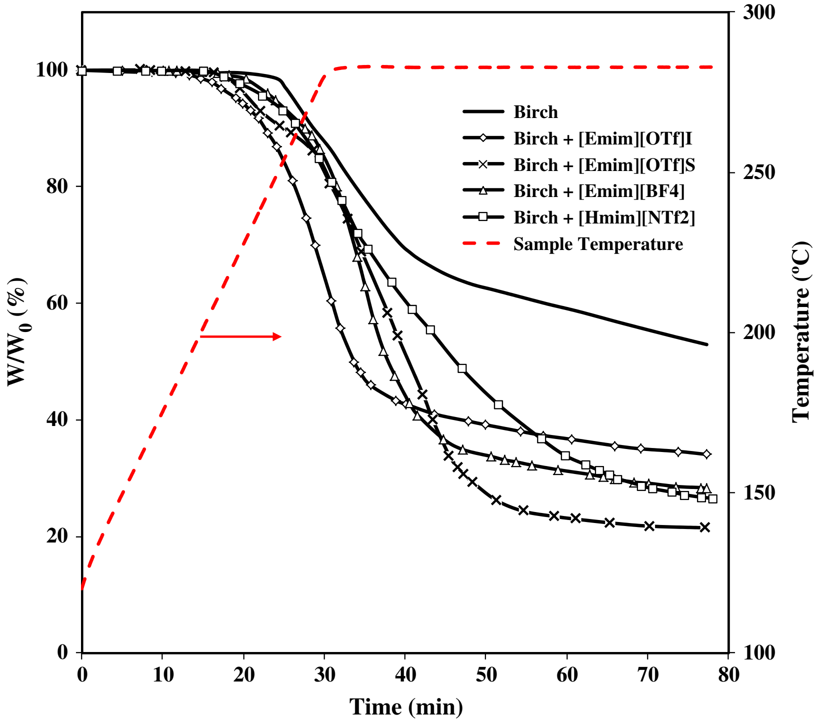

Fig. 8. Mass loss profile of birch wood ionic liquid and dry torrefaction.

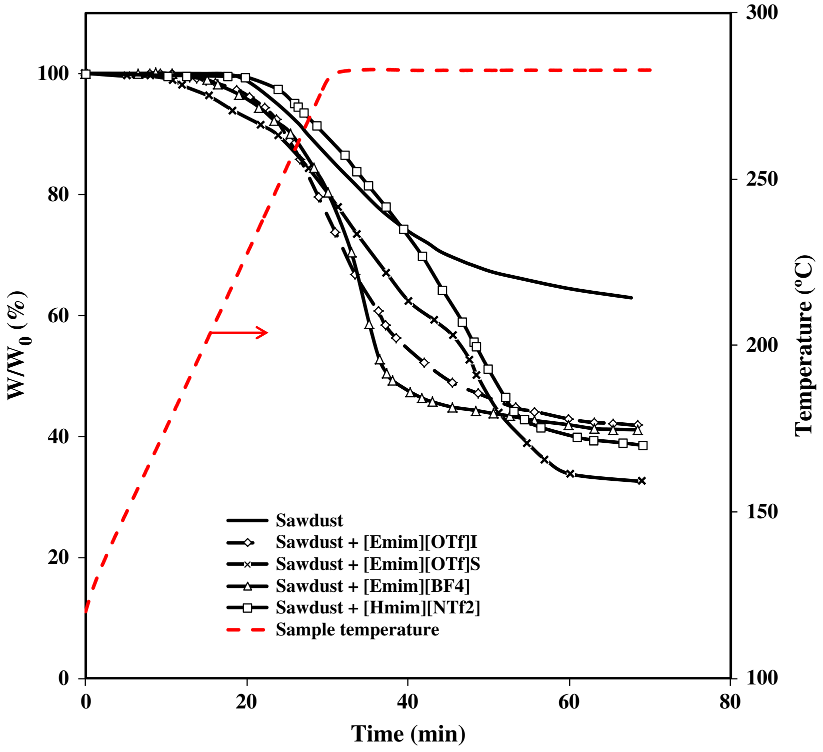

Fig. 9. Mass loss profile of sawdust ionic liquid and dry torrefaction.

scored as contact time and temperature increased from 30 to 60 min and 240–280 °C, respectively. These results are consistent with the increased decomposition rates of [Emim][OTf]$_S$-impregnated aspen, sawdust and birch as unveiled from above TG analysis. It can be inferred that IL-torrefaction of biomass may reduce to a large extent the residence time required to reach a certain biomass mass yield during torrefaction.

Results of elemental analysis of aspen, birch and sawdust before and after torrefaction are summarized in Table 2. Dry and [Emim][OTf]$_S$ torrefaction of aspen, birch and sawdust led to an

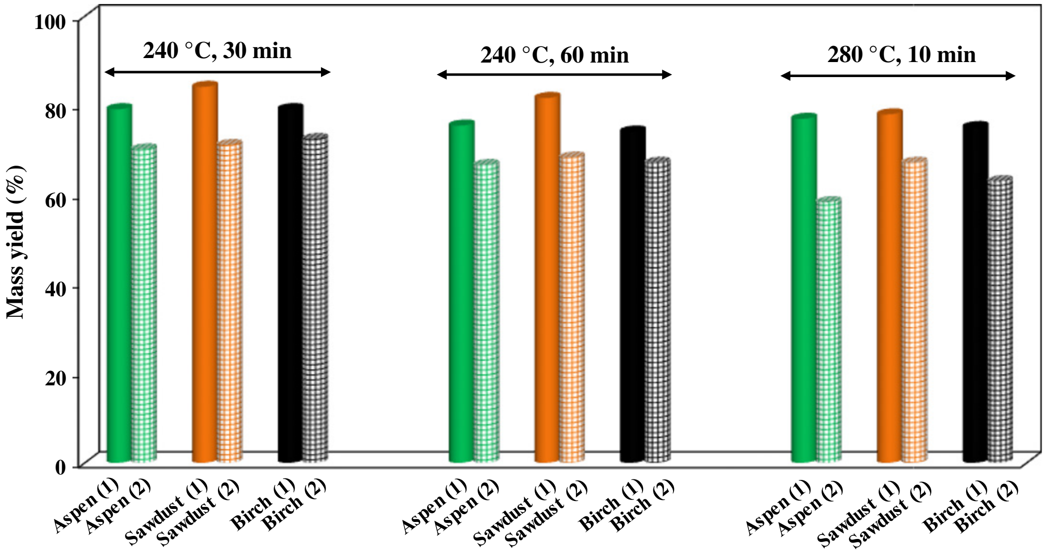

Fig. 10. Solid mass yield of torrefied aspen, birch and sawdust: (1) dry torrefaction, (2) ionic liquid ([Emim][OTf]$_S$) torrefaction.

increase in C/O ratio translating in an increase in energy density subsequent to biomass torrefaction. As shown in Fig. 11, the energy density, *e*, of aspen, birch and sawdust in all torrefied samples corresponding to Fig. 10 conditions exceeds 1.0 for both IL and dry torrefaction of biomass. The higher energy density of torrefied biomass as compared to raw aspen, birch and sawdust would vouch for lower shipping costs and superior performance of coal co-fired power plants [34]. The energy density of [Emim][OTf]$_S$-torrefied biomass was increased in the range 5–22% outperforming the *e* values corresponding to dry torrefaction which were limited between 3% and 9%.

Almost 90% of the non-condensable gases collected in the gas bag after cold trap were mostly composed of CO_2 for both [Emim][OTf]$_S$ and dry torrefaction of aspen, birch and sawdust while CO (7–8)% and methane (2–3)% were the other main constituents. In accordance with the ion current signals detected via MS, release of CO_2 and water during torrefaction could explain the increase in biomass C/O ratio and consequently leveraging of the heating value of the torrefied biomass samples, Table 2.

The energy yield, Y_e, of biomass torrefied with [Emim][OTf]$_S$ was below its dry torrefaction counterpart, everything else being kept constant. Fig. 12 compares the energy yield of IL torrefied aspen, birch and sawdust with dry torrefaction. This latter led to 1–25% higher energy yields than [Emim][OTf]$_S$-torrefied biomass. These results can be explained by the fast decomposition of aspen, birch and sawdust cellulose during [Emim][OTf]$_S$ torrefaction which may released tar compounds that contributed to a reduction of Y_e of IL torrefied biomass.

To assess hydrophobicity in the torrefied products, U_{MU} of solid products of [Emim][OTf]$_S$ and dry torrefaction of aspen, birch and

Table 2
Ultimate analysis, mass yield (dry basis) and high heating value of raw, and dry and ionic liquid ([Emim][OTf]$_S$) torrefied aspen, birch and sawdust at different residence time and temperatures.

	Raw biomass	240 °C, 30 min		240 °C, 60 min		280 °C, 10 min	
		Dry	Ionic liquid	Dry	Ionic liquid	Dry	Ionic liquid
Aspen							
C (mass%)	48.5	50.2	51.5	50.5	51.8	51.8	51.5
H (mass%)	6.9	6.6	6.0	6.3	6.3	6.3	5.9
O (mass%)	44.4	43.2	42.1	43.1	41.6	42.0	42.1
N (mass%)	0.02	0.03	0.45	0.07	0.36	0	0.33
Mass yield (%)		79.2	70.2	75.5	66.7	77	58.3
C/O	1.19	1.16	1.22	1.17	1.25	1.23	1.22
HHV (kJ/kg)	19,400	20,100	20,600	20,200	20,800	20,700	20,500
Birch							
C (mass%)	48.4	49.7	51.6	50.9	51.6	51.0	54.7
H (mass%)	6.9	6.6	5.8	6.4	6.4	6.3	5.0
O (mass%)	44.2	43.6	41.8	42.6	41.6	42.7	39.8
N (mass%)	0.06	0.09	0.42	0.08	0.40	0.06	0.44
Mass yield (%)		79.2	72.5	74.2	67.2	75.2	63.0
C/O	1.10	1.14	1.24	1.19	1.24	1.19	1.38
HHV (kJ/kg)	19,400	19,900	20,600	20,400	20,800	20,400	21,500
Sawdust							
C (mass%)	48.9	51.7	51.5	53.3	53.5	52.0	58.3
H (mass%)	6.4	6.2	6.0	5.8	4.8	5.8	5.5
O (mass%)	42.7	42.0	42.1	40.7	41.0	42.1	35.4
N (mass%)	0.06	0.19	0.47	0.18	0.69	0.05	0.77
Mass yield (%)		84.2	71.2	81.7	68.3	78.0	67.2
C/O	1.15	1.23	1.22	1.31	1.30	1.23	1.64
HHV (kJ/kg)	19,500	20,700	20,500	21,300	20,900	20,700	23,700

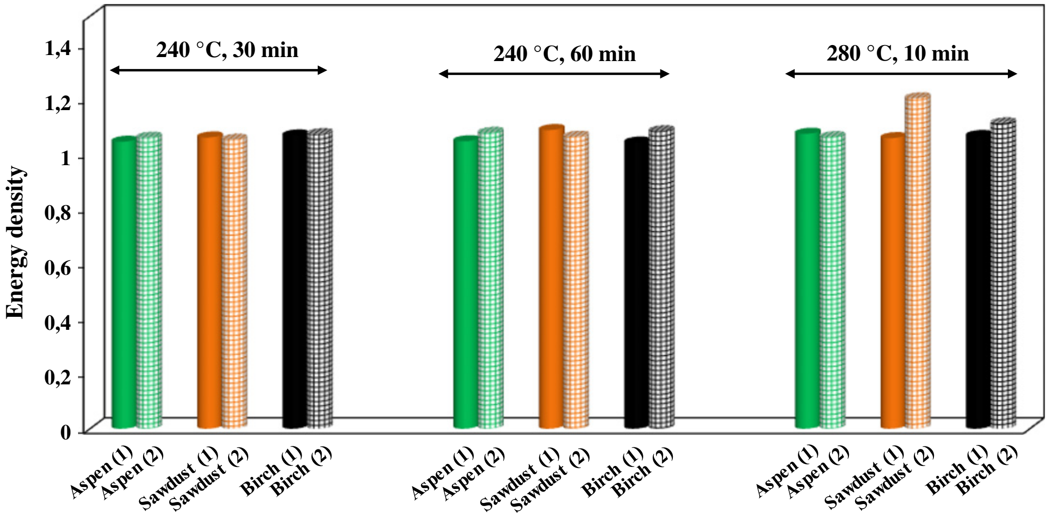

Fig. 11. Energy density of torrefied aspen, birch and sawdust: (1) dry torrefaction, and (2) ionic liquid ([Emim][OTf]$_S$) torrefaction.

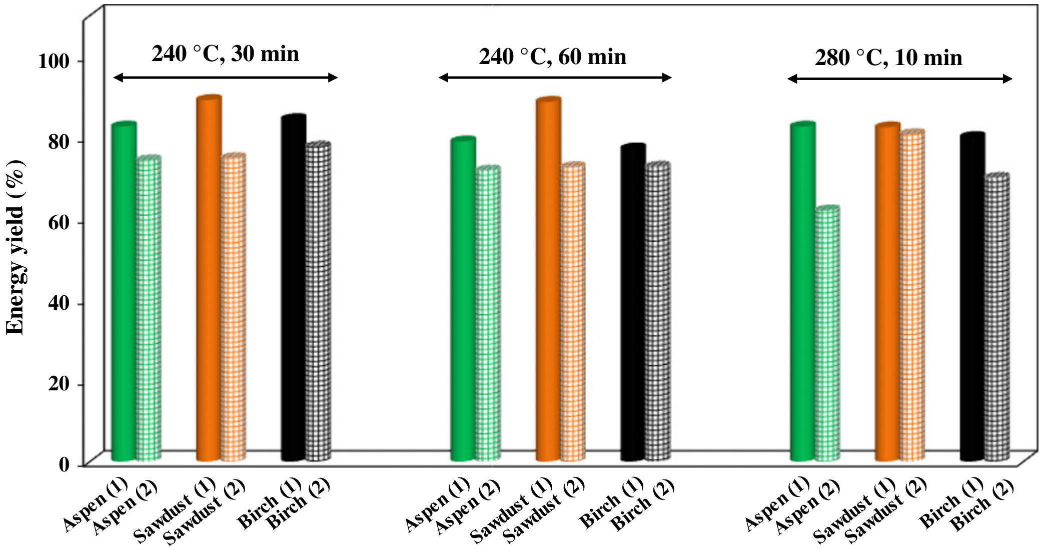

Fig. 12. Energy yield of torrefied aspen, birch and sawdust: (1) dry torrefaction, and (2) ionic liquid ([Emim][OTf]$_S$) torrefaction.

sawdust were also measured. To eliminate biological activity and biomass deterioration during storage and to maintain lower transportation fees, U_{MU} has to be kept as low as possible [7]. As seen in Table 3, U_{MU} of solid products after [Emim][OTf]$_S$ and dry torrefaction of aspen, birch and sawdust were considerably lower than their U_{MU} before torrefaction. Moisture uptake occurs through hydrogen bond with the hydroxyl groups of the lignocellulosic cell wall components [7]. However, these hydroxyl groups by breaking during torrefaction yield more hydrophobic solids [7]. IL torrefaction led to 40–45% reduction in U_{MU} as compared to raw aspen, birch and sawdust. However, in most experiments, dry torrefaction led to solid products with U_{MU} lower than [Emim][OTf]$_S$ torrefaction. Increasing temperature of biomass torrefaction from 240 to 280 °C improved hydrophobicity of aspen, birch and sawdust solid products. Such increase in hydrophobicity of aspen, birch and sawdust after IL torrefaction was also confirmed from contact angle measurements. The contact angle for raw aspen, birch and sawdust were 83.3°, 82.2° and 75.25°, respectively. Correspondingly, contact angle of [Emim][OTf]$_S$-torrefied aspen, birch and sawdust at 280 °C increased to 92.85°, 92.75° and 90.65°.

Table 3
Ultimate moisture uptake of raw, dry and ionic liquid ([Emim][OTf]$_S$) torrefied aspen, birch and sawdust at different residence time and temperatures after 4-day exposure of samples in saturated stream of 30 °C.

	Raw biomass	240 °C, 30 min		240 °C, 60 min		280 °C, 10 min	
		Dry	With IL	Dry	With IL	Dry	With IL
Aspen	24.8	15.5	17.4	15.7	16.7	14.1	14.3
Birch	23.9	15.3	16.1	14.0	16.7	15.4	13.4
Sawdust	22.6	15.6	16.3	15.6	15.9	13.6	13.5

Table 4
Decomposition rate (mass%/h) of different ionic liquids tested in this study at different operating conditions.

	[Emim][BF$_4$]	[Hmim][NTf$_2$]	[Emim][OTf]$_s$	[Emim][OTf]$_l$
As-received IL	0.93	0.63	0.37	0.47
IL + 2 wt.% ash	1.41	1.15	0.51	0.79
IL + 2 wt.% ash + 2 wt.% char	1.52	1.2	0.49	0.83

3.3. IL thermal stability under torrefaction conditions

Investigating the contributory factors for long-term stability of ionic liquids as implemented for biomass torrefaction is important to check. Although the onset decomposition temperature of [Emim][BF$_4$] [24], [Emim][OTf] [24] and [Hmim][NTf$_2$] [26] as obtained from fast TG scanning is in excess of 400 °C, other investigations have also revealed that decomposition of ILs may take place even at lower temperatures should they be employed over long-term periods [35]. Furthermore, production of some reactive gases during biomass thermal treatment as well as dissolution of biomass minerals may represent as many factors to catalyze ionic liquid decomposition [35]. Although imidazolium-based ionic liquids start to degrade, to some extent, at lower temperatures than those concluded from thermogravimetric analysis [36], long-term thermal stability of ionic liquid has been also studied via TG by several groups [35,37].

In this study, long term stability of ionic liquids is tested at 280 °C using coupled TG–MS analysis. IL samples were dried in TG at 120 °C for 30 min and then submitted to prograde heating at 5 °C/min until 280 °C. The samples were maintained overnight at this temperature to study their decomposition rate. The decomposition rate of as-received [Emim][OTf], [Emim][BF$_4$] and [Hmim][NTf$_2$] in a non-reactive gas environment (N$_2$) is shown in the first entry of Table 4. Fig. 13 also shows the TG trend of decomposition of the mentioned ionic liquids. These data unveil some degradation at low temperature in accordance with the long-term thermal stability studies below 400 °C. The decomposition rates of tested ILs follow the order: [Emim][BF$_4$] > [Hmim][NTf$_2$] > [Emim][OTf]. [Emim][OTf] from Sigma Aldrich had lower decomposition rate than that from ioli-tech as the acidic impurities present in the latter could prompt faster Emim cation decompositions [35].

Thermal pretreatment of biomass at 280 °C leads to the release of volatile and non-volatile gases such as organic acids, steam, CO$_2$, CO, CH$_4$ and a small amount of hydrogen [38]. To investigate the sensitivity of IL decomposition to the presence of gases evolving during biomass thermal treatment, the non-reactive N$_2$ environment in the TG chamber was replaced by binary mixtures of 10%/90% CO$_2$/N$_2$, CO/N$_2$, CH$_4$/N$_2$, H$_2$O/N$_2$ and steam/N$_2$. Although the decomposition rate of imidazolium based ionic liquids is reported to increase in the presence of air [35], our results showed no extensive changes in IL decomposition in response to changes in gas environments.

The effect of dissolution of minerals coexisting with biomass on the decomposition rate of the tested ionic liquids was also studied. Woody biomass contains some amounts of Si, Ca, K, Mg, P, Fe and Al [39] prone to dissolution in ILs during torrefaction. Dissolution of Fe, Au, Ag, Cu, Na and K, Mg and Ca in imidazolium-based ILs is known [40–42]. Mineral dissolution in ILs can be enhanced by elevated temperatures as in thermal treatment of biomass [40]. To investigate these effects on IL decomposition, ash was first produced after sawdust pyrolysis in the fixed bed at 800 °C and N$_2$ environment and then burning the residual carbon for 4 h at 800 °C. Addition of 2 wt.% of ash to ionic liquid affected considerably its decomposition rate. The decomposition rate of the tested ILs (Table 4) increased by up to 100% and confirms the prejudice of minerals due to ash leftover. It is consistent with the reported boost on decomposition rate of 1-alkyl-3-methylimidazolium triflates by amorphous and quartz silica [35], BF$_4$ anions by calcium [27] and imidazolium ILs containing inorganic fluoride anions such as PF$_6$ and BF$_4$ by aluminum [22]. Switching in the presence of ash the N$_2$ environment to gaseous mixtures to reflect the torrefaction evolving gases, i.e., 10%/90% CO$_2$/N$_2$, CO/N$_2$, CH$_4$/N$_2$, H$_2$O/N$_2$ and steam/N$_2$, had no boosting or neutralizing effect on IL decomposition.

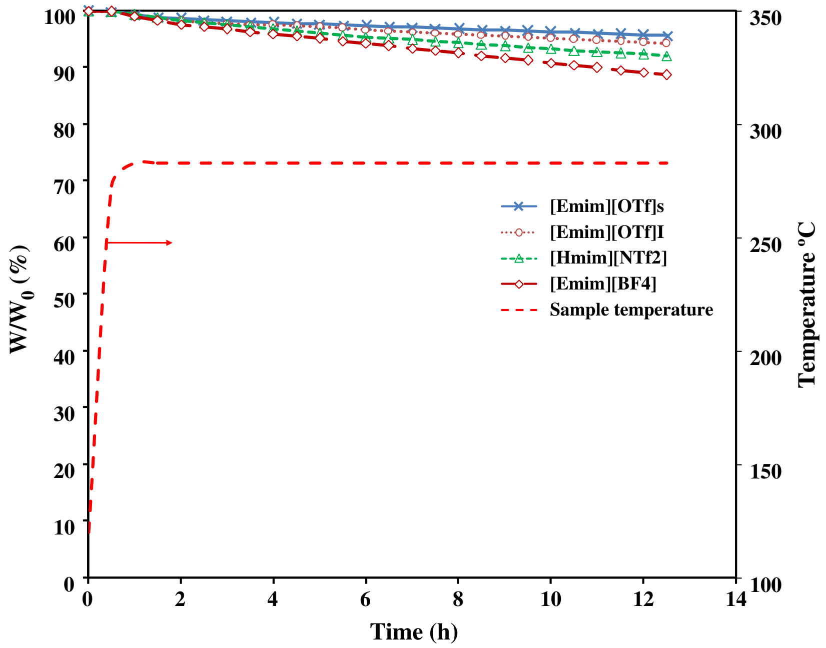

Fig. 13. TG profile of [Emim][OTf]S, [Emim][OTf]I, [Hmim][NTf2] and [Emim][BF4] heated from 120 °C to 280 °C with 5 °C/min heating rate and held at 280 °C for 12 h.

Contacting between IL, solid biochar and ash on IL decomposition rate was also studied. Biochar was mixed with ash and IL in the proportions 2 wt.%/2 wt.%/96 wt.%, respectively. Special care was paid for char generation since contacting between IL and char may lead to the production of some volatiles from char itself. Consequently, char was generated by overnight pyrolysis of sawdust in TG at 950 °C and under N_2 environment after heating the biomass with the maximum rate achievable by TG (200 °C/min) to extract the maximum volatiles from the sawdust. Addition of 2 wt.% of char to the mixtures of ionic liquid and ash led to small increase in the decomposition rates of [Emim][BF_4], [Hmim][NTf_2] and [Emim][OTf]$_l$ while it had no effect in case of [Emim][OTf]s, see Table 4. As previously, switching from N_2 to mixtures of 10%/90% of CO_2/N_2, CO/N_2, CH_4/N_2, H_2O/N_2 and steam/N_2, in the presence of ash and char at 280 °C had no incremental effect due to gas on the decomposition rate of tested ionic liquids.

4. Conclusion

Torrefaction of cellulose, hemicellulose and lignin, and three different woody biomass varieties, namely, aspen, birch and sawdust impregnated with different ionic liquids, namely, [Emim][BF_4], [Emim][OTf] and [Hmim][NTf_2] was studied. The thermal decomposition rate of cellulose was found to increase considerably due to [Emim][OTf] and [Emim][BF_4]. However, thermal decomposition of IL-torrefied xylan and lignin was comparable with dry torrefaction. For constant contact time and temperature, the decomposition rates of IL-impregnated birch, aspen and sawdust increased considerably compared to dry torrefaction. The efficiency of IL and dry torrefaction of aspen, birch and sawdust was compared in terms of mass yield, energy density, energy yield, hydrophobicity and ultimate moisture uptake of solid products. The energy density IL-torrefied biomass exceeded that of dry torrefaction. Conversely, plausibly ascribed to the release of heavy tars due to fast cellulose decomposition, the energy yield of IL-torrefied biomass was lower than dry torrefaction. Improvement in hydrophobicity of solid products from both IL and dry torrefaction was observed. This improvement led to nearly 40–45% reduction in ultimate moisture uptake of IL and dry torrefaction of aspen, birch and sawdust. Dissolution of minerals pre-existing in biomass have been shown to be detrimental in terms of prolonged exposures of ionic liquids and their possible degradation in the long run.

Acknowledgments

Support from the Natural Sciences and Engineering Research Council of Canada, the Canada Research Chair "Green processes for cleaner and sustainable energy", and the FQRNT-funded "Center in Green Chemistry & Catalysis" (CGCC) is gratefully acknowledged.

Appendix A. Supplementary material

Supplementary data associated with this article can be found, in the online version, at http://dx.doi.org/10.1016/j.fuel.2012.09.037.

References

[1] Berndes G, Hoogwijk M, van den Broek R. The contribution of biomass in the future global energy supply: a review of 17 studies. Biomass Bioenergy 2003;25:1–28.

[2] Chen WH, Kuo PC. Torrefaction and co-torrefaction characterization of hemicellulose, cellulose and lignin as well as torrefaction of some basic constituents in biomass. Energy 2011;36:803–11.

[3] Pimchuai A, Dutta A, Basu P. Torrefaction of agriculture residue to enhance combustible properties. Energy Fuel 2010;24:4638–45.

[4] Hoekman SK, Broch A, Robbins C. Hydrothermal Carbonization (HTC) of lignocellulosic biomass. Energy Fuel 2011;25:1802–10.

[5] Deng J, Wang GJ, Kuang JH, Zhang YL, Luo YH. Pretreatment of agricultural residues for co-gasification via torrefaction. J Anal Appl Pyrol 2009;86:331–7.

[6] Yan W, Hastings JT, Acharjee TC, Coronella CJ, Vasquez VR. Mass and energy balances of wet torrefaction of lignocellulosic biomass. Energy Fuel 2010;24:4738–42.

[7] Yan W, Acharjee TC, Coronella CJ, Vasquez VR. Thermal pretreatment of lignocellulosic biomass. Environ Prog Sustain 2009;28:435–40.

[8] Medic D, Darr M, Shah A, Potter B, Zimmerman J. Effects of torrefaction process parameters on biomass feedstock upgrading. Fuel 2012;91:147–54.

[9] Patel B, Gami B, Bhimani H. Improved fuel characteristics of cotton stalk, prosopis and sugarcane bagasse through torrefaction. Energy Sustain Dev 2011;15:372–5.

[10] Chen WH, Cheng WY, Lu KM, Huang YP. An evaluation on improvement of pulverized biomass property for solid fuel through torrefaction. Appl Energy 2011;88:3636–44.

[11] Prins MJ, Ptasinski KJ, Janssen F. Torrefaction of wood – Part 1. Weight loss kinetics. J Anal Appl Pyrol 2006;77:28–34.

[12] van der Stelt MJC, Gerhauser H, Kiel JHA, Ptasinski KJ. Biomass upgrading by torrefaction for the production of biofuels: a review. Biomass Bioenergy 2011;35:3748–62.

[13] Wang S, Liu Q, Luo Z, Wen L, Can K. Mechanism study on cellulose pyrolysis using thermogravimetric analysis coupled with infrared spectroscopy. Front Energy Power Eng China 2007;1:413–9.

[14] Tadesse H, Luque R. Advances on biomass treatment using ionic liquids: an overview. Energy Environ Sci 2011;4:3913–29.

[15] Julien S, Chornet E, Overend RP. Influence of acid pretreatment (H_2SO_4, HCl, HNO_3) on reaction selectivity in the vacuum pyrolysis of cellulose. J Anal Appl Pyrol 1993;27:25–43.

[16] Brodeur G, Yau E, Badal K, Collier J, Ramachandran KB, Ramakrishnan S. Chemical and physicochemical pretreatment of lignocellulosic biomass: a review. Enzyme Res 2011;2011. ID 787532.

[17] Li B, Asikkala J, Filpponen I, Argyropoulos DS. Factors affecting wood dissolution and regeneration of ionic liquids. Ind Eng Chem Res 2010;49:2477–84.

[18] Zakrzewska ME, Bogel-Lukasik E, Bogel-Lukasik R. Solubility of carbohydrates in ionic liquids. Energy Fuel 2010;24:737–45.

[19] Van Valkenburg ME, Vaughn RL, Williams M, Wilkes JS. Thermochemistry of ionic liquid heat-transfer fluids. Thermochim Acta 2005;425:181–8.

[20] Maki-Arvela P, Anugwom I, Virtanen P, Sjoholm R, Mikkola JP. Dissolution of lignocellulosic materials and its constituents using ionic liquids – a review. Ind Crop Prod 2010;32:175–201.

[21] Sun N, Rodriguez H, Rahman M, Rogers RD. Where are ionic liquid strategies most suited in the pursuit of chemicals and energy from lignocellulosic biomass? Chem Commun 2011;47:1405–21.

[22] Ngo HL, LeCompte K, Hargens L, McEwen AB. Thermal properties of imidazolium ionic liquids. Thermochim Acta 2000;357:97–102.

[23] Fredlake CP, Crosthwaite JM, Hert DG, Aki S, Brennecke JF. Thermophysical properties of imidazolium-based ionic liquids. J Chem Eng Data 2004;49:954–64.

[24] Huddleston JG, Visser AE, Reichert WM, Willauer HD, Broker GA, Rogers RD. Characterization and comparison of hydrophilic and hydrophobic room temperature ionic liquids incorporating the imidazolium cation. Green Chem 2001;3:156–64.

[25] Lee SH, Dang DT, Ha SH, Chang WJ, Koo YM. Lipase-catalyzed synthesis of fatty acid sugar ester using extremely supersaturated sugar solution in ionic liquids. Biotechnol Bioeng 2008;99:1–8.

[26] Crosthwaite JM, Muldoon MJ, Dixon JK, Anderson JL, Brennecke JF. Phase transition and decomposition temperatures, heat capacities and viscosities of pyridinium ionic liquids. J Chem Thermodyn 2005;37:559–68.

[27] Katagiri J, Borjigin S, Yoshioka T, Mizoguchi T. Formation and decomposition of tetrafluoroborate ions in the presence of aluminum. J Mater Cycles Waste 2010;12:136–46.

[28] Friedl A, Padouvas E, Rotter H, Varmuza K. Prediction of heating values of biomass fuel from elemental composition. Anal Chim Acta 2005;544:191–8.

[29] Bridgeman TG, Jones JM, Shield I, Williams PT. Torrefaction of reed canary grass, wheat straw and willow to enhance solid fuel qualities and combustion properties. Fuel 2008;87:844–56.

[30] Bridgeman TG, Jones JM, Williams A, Waldron DJ. An investigation of the grindability of two torrefied energy crops. Fuel 2010;89:3911–8.

[31] Antal M, Simkovic I, Ebringerova A, Micko MM. New aspects in cationization of lignocellulose materials. 4. Modification of aspen wood meal with quarternary ammonium groups. J Appl Polym Sci 1986;31:621–5.

[32] Li C, Zheng M, Wang A, Zhang T. On-pot catalytic hydrocracking of woody biomass into chemicals over supported carbide catalysts: simultaneous conversion of cellulose hemicellulose and lignin. Energy Environ Sci 2011.

[33] Radmanesh R, Courbariaux Y, Chaouki J, Guy C. A unified lumped approach in kinetic modeling of biomass pyrolysis. Fuel 2006;85:1211–20.

[34] Phanphanich M, Mani S. Impact of torrefaction on the grindability and fuel characteristics of forest biomass. Bioresource Technol 2011;102:1246–53.

[35] Kosmulski M, Gustafsson J, Rosenholm JB. Thermal stability of low temperature ionic liquids revisited. Thermochim Acta 2004;412:47–53.

[36] Meine N, Benedito F, Rinaldi R. Thermal stability of ionic liquids assessed by potentiometric titration. Green Chem 2010;12:1711–4.

[37] Seeberger A, Andresen AK, Jess A. Prediction of long-term stability of ionic liquids at elevated temperatures by means of non-isothermal thermogravimetrical analysis. Phys Chem Chem Phys 2009;11:9375–81.

[38] Prins MJ, Ptasinski KJ, Janssen F. Torrefaction of wood – Part 2. Analysis of products. J Anal Appl Pyrol 2006;77:35–40.
[39] Masia AAT, Buhre BJP, Gupta RP, Wall TF. Characterising ash of biomass and waste. Fuel Process Technol 2007;88:1071–81.
[40] Whitehead JA, Zhang J, Pereira N, McCluskey A, Lawrance GA. Application of 1-alkyl-3-methyl-imidazolium ionic liquids in the oxidative leaching of sulphidic copper, gold and silver ores. Hydrometallurgy 2007;88:109–20.
[41] Chun S, Dzyuba SV, Bartsch RA. Influence of structural variation in room-temperature ionic liquids on the selectivity and efficiency of competitive alkali metal salt extraction by a crown ether. Anal Chem 2001;73:3737–41.
[42] Bartsch RA, Chun S, Dzyuba SV. Ionic liquids as novel diluents for solvent extraction of metal salts by crown ethers. In: Rogers RD, Seddon KR, editors. Ionic liquids: industrial applications for green chemistry, vol. 818. Washington: Amer Chemical Soc.; 2003.